



# Effect of carbon defects on the nitrogen-doped carbon catalytic performance for acetylene hydrochlorination



Jian Wang<sup>a</sup>, Wanqi Gong<sup>a</sup>, Mingyuan Zhu<sup>a,b,\*</sup>, Bin Dai<sup>a,b</sup>

<sup>a</sup> School of Chemistry and Chemical Engineering of Shihezi University, Shihezi, Xinjiang 832000, PR China

<sup>b</sup> Key Laboratory for Green Processing of Chemical Engineering of Xinjiang Bingtuan, Shihezi, Xinjiang 832000, PR China

## ARTICLE INFO

### Keywords:

Nitrogen-doped carbon  
Acetylene hydrochlorination  
Carbon defect  
Catalytic performance

## ABSTRACT

The carbon defects in nitrogen-doped carbon were controlled by removing the N atoms under different temperatures during the catalyst preparation process. The synthesised catalysts were characterised by multiple techniques, and the catalytic performance was evaluated under experimental conditions of gas hourly space velocity ( $C_2H_2$ ) =  $36\text{ h}^{-1}$  at  $220\text{ }^\circ\text{C}$ . The catalytic performance of the synthesised nitrogen-doped carbon for acetylene hydrochlorination increased with the increment of carbon defect. Carbon defects in the catalysts were proposed to affect the adsorption of  $C_2H_2$  and HCl and promote their conversion. The regeneration of the nitrogen-doped carbon catalyst was found to be effective by using high-temperature treatment in an  $NH_3$  atmosphere.

## 1. Introduction

Acetylene hydrochlorination is a very important method for manufacturing vinyl chloride monomer (VCM) in China because China contains rich deposits of coal but lacks oil. However, the industrial catalyst for acetylene hydrochlorination is  $HgCl_2$ , which is toxic to the human body and the environment [1]. Therefore, the exploitation of environmentally friendly non-mercury catalysts is attracting increasing attention for acetylene hydrochlorination.

In the past decades, Au catalysts have been found to be effective for acetylene hydrochlorination. In our previous work, we designed an Au catalyst whose acetylene conversion rate reached 100%. This catalyst could be stably used for 6513 h under industrial application conditions [2,3]. Wei et al. [4] found that a Au catalyst with thiocyanate ligands could operate for over 3000 h in a 4 t per annum scale pilot experiment. Hutchings et al. [5] reported very exciting results for the development of non-mercury acetylene hydrochlorination catalysts. By using thio ligands as soft donor atoms, active  $Au^+$  and  $Au^0$  were present consistent with the formation and deposition of Au catalyst, and the synthesised catalyst could last over 3000 kg VCM/kg catalyst, which is a very low Au loading. These investigations greatly accelerated the commercialisation of non-mercury catalysts for acetylene hydrochlorination. However, given the high cost and scarcity of Au, low-cost catalysts are being sought as non-mercury replacement catalysts for acetylene hydrochlorination.

In our previous work, we synthesised  $C_3N_4$  for acetylene hydrochlorination, and we found that the acetylene conversion rate of this catalyst can reach 75% of the  $HgCl_2$  catalyst efficiency. According to density functional theory (DFT) calculations, carbon atoms were the adsorption sites for acetylene, and nitrogen atoms were the adsorption sites for hydrogen chloride [6]. The reaction activation energy was  $77.94\text{ kcal/mol}$ , which is much higher than  $AuCl_3$  ( $11.9\text{ kcal/mol}$ ) [7]. Thereafter, many groups have synthesised catalysts with nitrogen-doped carbons that display excellent catalytic performance. Wei et al [8]. reported nitrogen-doped carbon nanotubes that could greatly enhance the adsorption of acetylene. This catalyst showed excellent catalytic properties with turn over frequency (TOF) of up to  $2.3 \times 10^{-3}/s$ . Pan et al. [9] found that the catalyst activity increased with increasing N content, and only carbon atoms linked to pyrrolic nitrogen could adsorb acetylene. Thus, they found that the type of nitrogen played a major role in this reaction. The catalyst performance stabilised at above 80% under 30/h ( $C_2H_2$ ) and  $200\text{ }^\circ\text{C}$  during 150 h. In our previous work, we considered the effect of the nitrogen species in the nitrogen-doped catalyst for acetylene hydrochlorination and found that the effectiveness of the nitrogen species for acetylene hydrochlorination followed this order: pyrrolic N > graphitic N > pyridinic N [10]. On the basis of that sequence, we then designed and synthesised boron and nitrogen dual-doped graphene (B, N-G) materials. The acetylene conversion on that catalyst could reach to 95%, which was very close to the performance of Au and Hg catalysts [11].

\* Corresponding author at: School of Chemistry and Chemical Engineering of Shihezi University, Shihezi, Xinjiang 832000, PR China.

E-mail address: [zhuminyuan@shzu.edu.cn](mailto:zhuminyuan@shzu.edu.cn) (M. Zhu).

<https://doi.org/10.1016/j.apcata.2018.07.025>

Received 21 May 2018; Received in revised form 15 July 2018; Accepted 17 July 2018

Available online 18 July 2018

0926-860X/ © 2018 Elsevier B.V. All rights reserved.

Although obvious progress has been made in carbon-based catalysts for acetylene conversion, it must be noted that the TOF on a single active site of the carbon-based catalyst is still much lower than that of an Au or Hg catalyst [11], and the stability of the carbon-based catalyst still needs improvement. In designing and synthesising carbon-based catalyst with better activity and stability, it is important to find the relationship between the physical properties and catalytic performance. Carbon defects in nitrogen-doped carbon can significantly affect the catalytic activity of the oxygen reduction reaction [12–14]. Therefore, we were extremely curious if carbon defects in our carbon-based catalyst may also affect the catalytic performance for acetylene hydrochlorination. Therefore, we investigated the adsorption ability of C<sub>2</sub>H<sub>2</sub> and HCl on mono-vacancy graphene, di-vacancy graphene and stone-wales defect graphene by using DFT calculations. We found that carbon defects could enhance the adsorption capacity for C<sub>2</sub>H<sub>2</sub> and HCl [15]. In this work, we controlled the synthesis of carbon defects during nitrogen-doped carbon synthesis by removing N atoms under high temperature and characterised the carbon defects by using X-ray photoelectron spectroscopy (XPS) and Raman spectroscopy. The catalytic performance was evaluated using a fixed-bed reactor. Temperature-programmed decomposition (TPD) experiments were used to characterise the reactant adsorption on the surface of the catalyst. Furthermore, the influence of defect on the N-doped carbon was elucidated by DFT calculations.

## 2. Experimental

### 2.1. Catalyst preparation

All materials, unless otherwise specified, were obtained from Aldrich Chemical Co. C<sub>2</sub>H<sub>2</sub> (acetylene gas, 99%) and HCl (hydrogen chloride gas, 99%) were used in this study. The catalysts were synthesised by following the procedure reported in Refs [16,17]. (i) 2,4,6-Tris(p-nitroanilino)-1,3,5-triazine was obtained as follows: cyanuric chloride (2.31 g), p-nitroaniline (8.65 g) and K<sub>2</sub>CO<sub>3</sub> (10.4 g) were added into 1,4-dioxane (120 ml). After refluxing for 24 h, the products were sequentially washed with deionised water, methanol and benzene and then filtered and dried under vacuum overnight. (ii) 2,4,6-Tris(p-aminoanilino)-1,3,5-triazine was then synthesised. SnCl<sub>2</sub>·2H<sub>2</sub>O (~20.7 g) was dissolved in HCl solution (12 M, 30 ml). The obtained 2,4,6-tris(p-nitroanilino)-1,3,5-triazine (4.89 g in 20 ml ethanol) was added in the above solution slowly and then refluxed for 48 h. After filtration, the resulting solid was re-dissolved in hot water; the pH was adjusted to 12 by using NaOH solution; and the precipitated product was sequentially washed with deionised water and methanol, filtered and then dried under vacuum overnight. (iii) Terephthaldehyde (50 mg), 2,4,6-tris(p-aminoanilino)-1,3,5-triazine (100 mg), anhydrous dioxane (5 ml) and aqueous acetic acid (3 M, 2 ml) were added to a Teflon-lined stainless steel autoclave. This was placed in an oven and kept at 120 °C for 7 d. The obtained powder was Soxhlet extracted in anhydrous THF for 72 h, dried at room temperature for 12 h and then dried at 70 °C for 2 h. A yellow powder was obtained after this sequence. (iv) The pyrolysis step was conducted at 700 °C, 900 °C and 1100 °C in N<sub>2</sub> atmosphere for 5 h at a ramp rate of 2 °C/min. Thereafter, the sample was degassed for 24 h at 180 °C. The catalysts were labelled C700, C900 and C1100.

### 2.2. Catalyst characterisation

XRD data were collected using a Bruker advanced D8 X-ray diffractometer using Cu-K $\alpha$  irradiation ( $\lambda = 1.5406 \text{ \AA}$ ) at 40 kV and 40 mA in the  $2\theta$  scanning range of 10° to 90°. Raman spectra were collected using a Horiba Jobin Yvon LabRAM HR800 (633 nm laser excitation). Thermogravimetric analysis was conducted using a TGDSC simultaneous thermal analyser (Netzsch Sta 449F3 Jupiter1, Germany). XPS data were collected using a Thermo ESCALAB 250XI with Al, Ka X-ray source (225 W). TPD was recorded with an AutoChem 2720

instrument (Micromeritics Instrument Corporation, USA), and the ramp rate was 10 °C/min, the flow rate was 40 ml/min under Ar atmosphere. The experiments were carried out over a temperature ramp of 25 – 600 °C, ramp rate of 10 °C/min, and flow rate of 40 ml/min under nitrogen atmosphere.

### 2.3. Description of catalytic tests and analytical criteria

The catalyst performance was evaluated using a fixed-bed micro-reactor (inner diameter: 10 mm). A CKW-1100 temperature controller was used to control the temperature. The air in the microreactor with catalyst (0.5 g, 2 ml) was replaced with nitrogen prior to commencing the reaction. Acetylene gas (1.2 ml/min) and hydrogen chloride (1.3 ml/min) were pumped into the reactor at a gas hourly space velocity (GHSV, C<sub>2</sub>H<sub>2</sub>) of 36/h, and the reaction temperature was 220 °C. A GC2014C with a FID (flame ionization detector) detector was used to analyse the reaction products. The conversion of acetylene (XA) and the selectivity of the catalyst to VCM (SVC) were calculated as follows:

$$X_A = (\Phi_{A0} - \Phi_A) / \Phi_{A0} \times 100\%,$$

$$S_{VC} = \Phi_{VC} / (\Phi_{A0} - \Phi_A) \times 100\%,$$

Where  $\Phi_{A0}$  is the volume fraction of acetylene in the raw gas,  $\Phi_A$  is the volume fraction of remaining acetylene in the product gas and  $\Phi_{VC}$  is the volume fraction of vinyl chloride in product gas. The catalytic performance was further evaluated by TOF, which was calculated using the following equation.<sup>11</sup>

$$\text{TOF} = \frac{n_{C_2H_2}}{n_N \cdot t}$$

Where  $n_N$  is the amount of substance of nitrogen atom in the catalyst,  $t$  is the reaction time, and  $n_{C_2H_2}$  is the amount of substance of C<sub>2</sub>H<sub>2</sub> in the time.

The adsorption behaviours was calculated by density functional theory (DFT) on catalyst. Gaussian09 software package was used to perform simulations [18]. The method is hybrid density functional method M062X [19]. In order to obtain more accurately results, a van der Waals energy correction has been applied by using the parameters defined by Grimme et al [20]. The cc-pVDZ basis set was applied for all atoms [21,22]. This basis set has been previously applied to produce reliable results in similar system [23]. The adsorption energy of HCl and C<sub>2</sub>H<sub>2</sub> adsorbed on catalyst was calculated as :

$$E = E_{\text{system}} - E_{\text{adsorbates}} - E_{\text{catalyst}}$$

$E$  is the adsorption energy;  $E_{\text{system}}$  is the total energy of adsorption complex;  $E_{\text{adsorbates}}$  the total energy of isolated adsorbates;  $E_{\text{catalyst}}$  is the energy of isolated catalyst.

## 3. Results and discussion

Fig. 1 shows the XRD patterns of the C700, C900 and C1100 catalysts. Two obvious distinct diffraction planes were found at 23° and 43°, corresponding to the (0 0 2) and (1 0 1) diffraction planes of graphitic carbon [24]. The XRD patterns reveal no other impurities, thus indicating that the nitrogen-doped carbon materials were synthesised and the predecessor materials were carbonised. Nitrogen adsorption/desorption isotherms was used to analyze the physical structures of catalysts. The results of the total pore volumes and specific areas were listed in Table 1. The result shows that all catalysts were mesoporous material.

During carbonisation, the loss of nitrogen atoms could form single-atom vacancies. Owing to the instability of a single-atom vacancy, two vacancies will combine to form divacancies. Divacancies include one octagon and two pentagons, which is usually treated as a G585 carbon defect (a topological defect which was combined by two pentagons and one octagonal). If the loss of the nitrogen atom becomes greater, more carbon defects are produced [16,25–27]. Table 2 lists the elemental

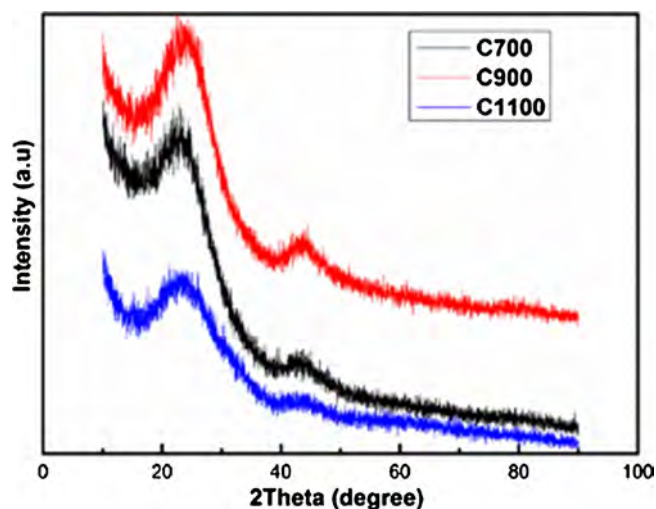


Fig. 1. XRD patterns of: C700, C900 and C1100.

**Table 1**  
Texture parameters of catalysts.

Sample	$S_{\text{BET}}$ ( $\text{m}^2 \text{g}^{-1}$ )	$V$ ( $\text{cm}^3 \text{g}^{-1}$ )	$D$ (nm)
C700	289.5	0.09	9.3
C900	265.9	0.09	10.9
C1100	294.5	0.10	9.6

**Table 2**  
Element composition of C700 C900 and C1100 catalysts determined by XPS.

Sample	Element Composition (%)		
	C	N	O
C700	89.46	7.00	3.54
C900	90.40	6.04	3.56
C1100	95.53	2.35	2.12

composition of the C700, C900 and C1100 catalysts. No obvious changes in the carbon and oxygen contents were observed while the nitrogen content was reduced from 7.00 to 2.35 as the carbonisation temperature increased from 700 °C to 1100 °C. This indicates that more nitrogen can leach at higher temperatures during the nitrogen-doped carbon catalyst preparation process, consistent with the literature [10]. Carbonisation temperature can also affect the types of nitrogen

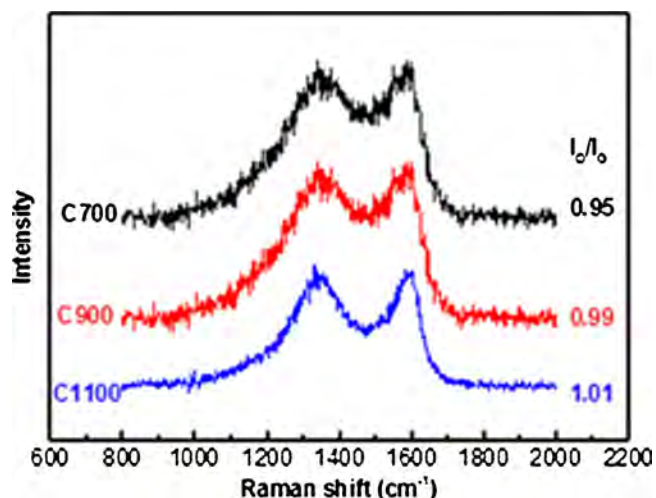


Fig. 3. Raman spectra of: C700, C900 and C1100.

obtained. The prepared C700, C900 and C1100 catalysts were analysed by XPS. As shown in Fig. 2a, there were three types of nitrogen: pyridinic nitrogen, pyrrolic nitrogen and graphitic nitrogen with binding energies at  $398.6 \pm 0.3$ , 400.4 eV and 401.2 eV, respectively [28,29]. We also analysed the relative atomic percentage of these three types of nitrogen in the obtained catalysts. As shown in Fig. 2b, the content for all three types of nitrogen decreased with increasing carbonisation temperature.

To investigate the degree of carbon defect formation in C700, C900 and C1100, Raman experiments were conducted. As shown in Fig. 3, there were two obvious bands at 1350 and 1588  $\text{cm}^{-1}$  that correspond to the D and G bands, respectively [30]. The ratio of  $I_{\text{D}}/I_{\text{G}}$  linearly increased from 0.95 to 1.01 with increasing carbonisation temperature. The carbon defects and disorders were generally illustrated by the D band and the carbon atom vibration mode. The graphite sheet vibration mode is represented by the G band. This indicates that more defects were synthesised under higher temperatures, consistent with the literature [31–34]. Combined with the results of XPS, it can be concluded that higher temperatures resulted in the loss of nitrogen atoms and produced more carbon defects in the nitrogen-doped carbon catalyst.

The TEM images and SAED pattern of C1100 catalyst were listed in Fig. 4, the structure and the morphology of C1100 catalyst could be easily analyzed, as Fig. 4 shows, this material with transparent and plicate morphology was similar with graphene and the SAED pattern (Fig. 4c) from the same area manifested the typical pattern

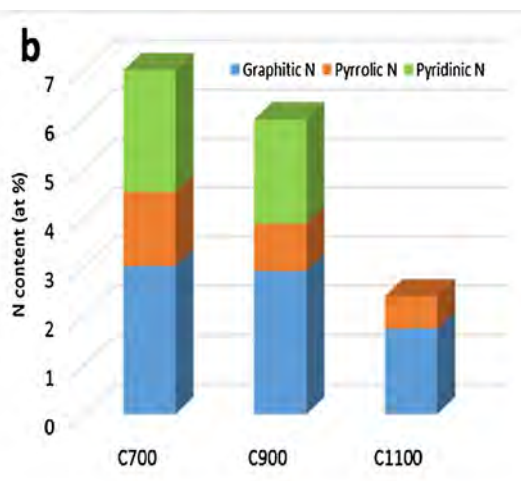
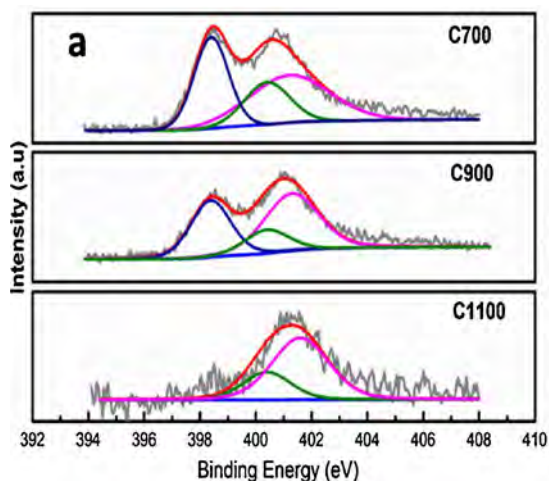


Fig. 2. (a): XPS deconvolution of N 1s for catalysts. (b): Relative atomic percentage of different nitrogen bonding states.

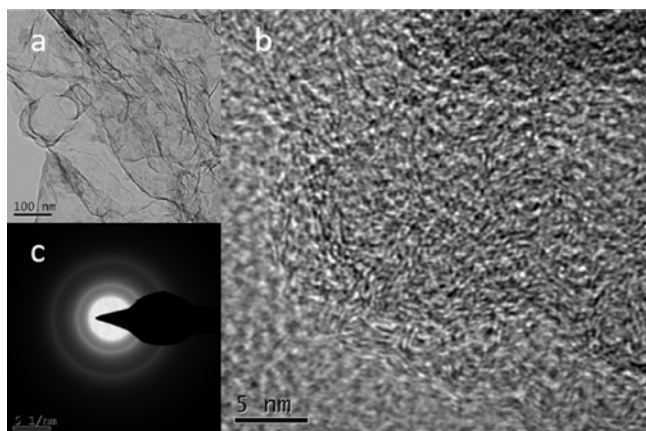


Fig. 4. TEM images and SAED pattern (insert) of C1100.

corresponded to polycrystalline materials.

The catalytic performance of catalysts for acetylene hydrochlorination was tested in a fixed-bed reactor under the following conditions: GHSV ( $C_2H_2$ ) of 36/h at 220 °C. The selectivity for all three catalysts was over 99%. Fig. 5a shows the acetylene conversions of C700, C900 and C1100 were 87.5%, 90.75% and 95.4%, respectively. It must be noted that the catalytic activity of C1100 was only a little lower than that of an Au catalyst and much higher than the results reported in our previous work (GHSV $_{C_2H_2}$  = 220 h $^{-1}$ , T = 180 °C, 92.24%) [1]. These results demonstrate that the catalytic activity of nitrogen-doped carbon becomes higher with increasing carbonisation temperature. However, the nitrogen content can also affect the catalytic performance of the nitrogen-doped carbon catalyst [10]. To clarify the effect of carbon defect on the catalytic performance for acetylene hydrochlorination, we calculated the TOF of C700, C900 and C1100 on the basis of the nitrogen content and initial acetylene conversion rates. As shown in Fig. 5b, the TOFs of C700, C900 and C1100 were  $1.89 \times 10^{-2}$  /min,  $2.24 \times 10^{-2}$  /min and  $6.10 \times 10^{-2}$  /min, respectively. In our previous work, the TOFs of g-C $_3$ N $_4$ /AC and B, N-G were  $1.42 \times 10^{-2}$  /min and  $3.32 \times 10^{-2}$  /min [35,11], respectively, and those results were much lower than the nitrogen-carbon catalysts reported in this work. As seen in Fig. 4b, the TOF was higher when more carbon defects were present. These results indicate that the existence of the defects effectively improved the catalytic activity for acetylene hydrochlorination.

To elucidate why carbon defects in the obtained nitrogen-doped carbon can enhanced the catalytic activity, TPD was used to

characterise the adsorption capacity of hydrogen chloride and acetylene on the surface of the C700, C900 and C1100 catalysts. The catalysts were loaded into the reactor, then acetylene gas or hydrogen chloride (20 ml/min) was pumped into the reactor at the reaction temperature was 220 °C for 2 h. As shown in Fig. 6, the obvious peaks at about 150 °C were assigned to the adsorption of HCl, and the peaks at 200 °C corresponded to the adsorption of  $C_2H_2$ . It can be seen that desorption peak areas of the HCl and  $C_2H_2$  both increased as carbon defects increased. C1100 displayed the largest desorption peak area, thus indicating that C1100 may possess the most active sites of these three samples. Combined with the XPS, Raman characterisation and TOF results, it can be concluded that the adsorption capacity of  $C_2H_2$  and HCl increased with increasing of carbon defects in the nitrogen-doped carbon, thereby promoting acetylene conversion in acetylene hydrochlorination.

The adsorption ability of N-doped carbon (PG-N) and N-doped defect carbon (DVG-N) on  $C_2H_2$  and HCl was also analyzed by DFT calculation, and there are two types of nitrogen (N1, N2) on DVG-N, nitrogen atoms which is near the defect was named as N1, nitrogen atoms which is away from the defect was named as N2, accordingly, the models were named as DVG-N1 and DVG-N2. The models employed were displayed in Fig. 7. The corresponding most stable adsorption structures of HCl and  $C_2H_2$  were shown in Figs. 8 and 9, respectively. Nitrogen atom is the adsorption site for HCl, and carbon atom is the adsorption site for  $C_2H_2$  in those catalysts, being consistent with our previous results [11].

Table 3 listed the difference of adsorption energies between PG-N and DVG-N. The adsorption energies ( $E_{ads}$ ) of HCl and  $C_2H_2$  on PG-N are  $-3.24$  and  $-4.61$  kcal/mol, respectively. Compared with PG-N, the adsorption ability of  $C_2H_2$  and HCl on DVG-N were significantly enhanced. The  $E_{ads-C_2H_2}$  of DVG-N1/ N2 were increased to  $-6.45$ ,  $-5.89$  kcal/mol, and The  $E_{ads-HCl}$  of DVG-N1/N2 were increased to  $-5.55$ ,  $-5.07$  kcal/mol, respectively. These results indicate that the existence of the defects effectively enhance the adsorption of HCl and  $C_2H_2$ , being consistent with the TPD results as Fig. 6 shown.

Given that the C1100 catalyst exhibited the best catalytic activity for acetylene hydrochlorination, we further investigated its stability under the experimental conditions of GHSV ( $C_2H_2$ ) = 36/h and 220 °C. Fig. 10a shows the acetylene conversion of C1100 decreased from 95.44% to 74.84% after running for 14 h, thus indicating that the synthesised C1100 catalyst does not have excellent stability. To understand the deactivation of C1100, TGA was conducted to characterise the coke deposition under an oxygen atmosphere. The calculation method for carbon deposition was the weight loss of used catalysts minus the weight of fresh catalyst in an appropriate temperature range,

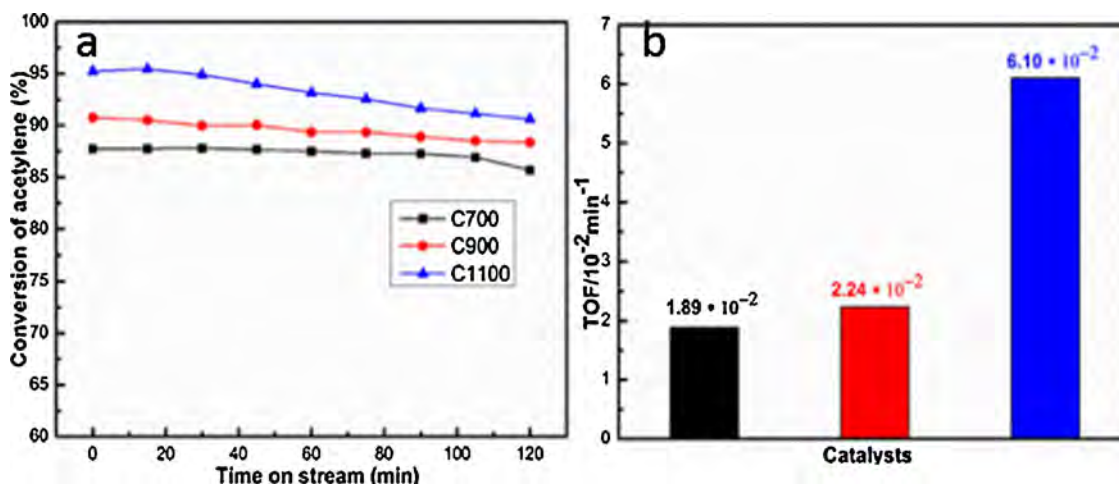


Fig. 5. (a): The acetylene conversion of C700, C900, and C1100 catalysts under GHSV of 36 h $^{-1}$  ( $C_2H_2$ ) and 220 °C for acetylene hydrochlorination; (b): The TOFs of C700, C900, C1100 catalysts based on single nitrogen atoms.

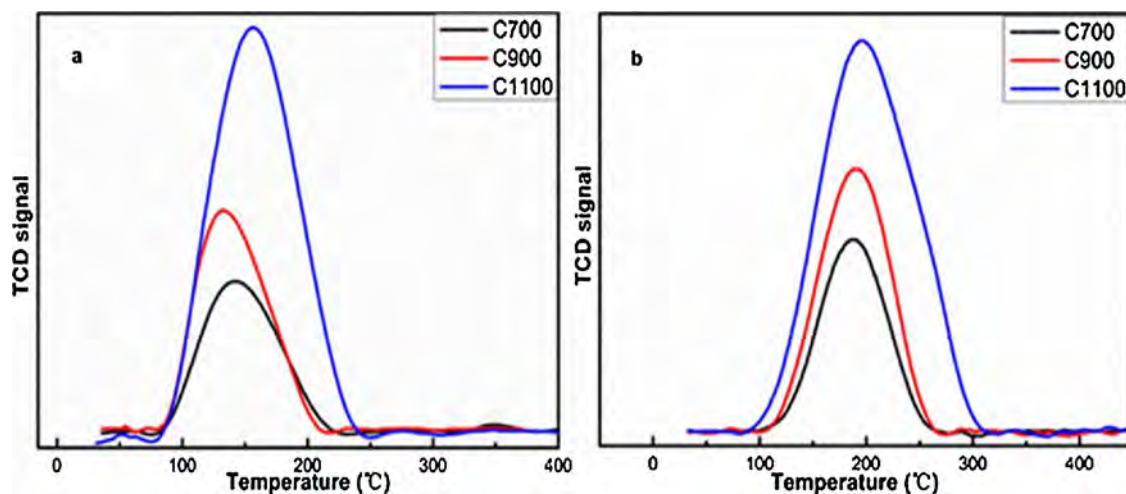


Fig. 6. TPD evolution profiles of catalysts: (a)  $C_2H_2$ ; (b) HCl.

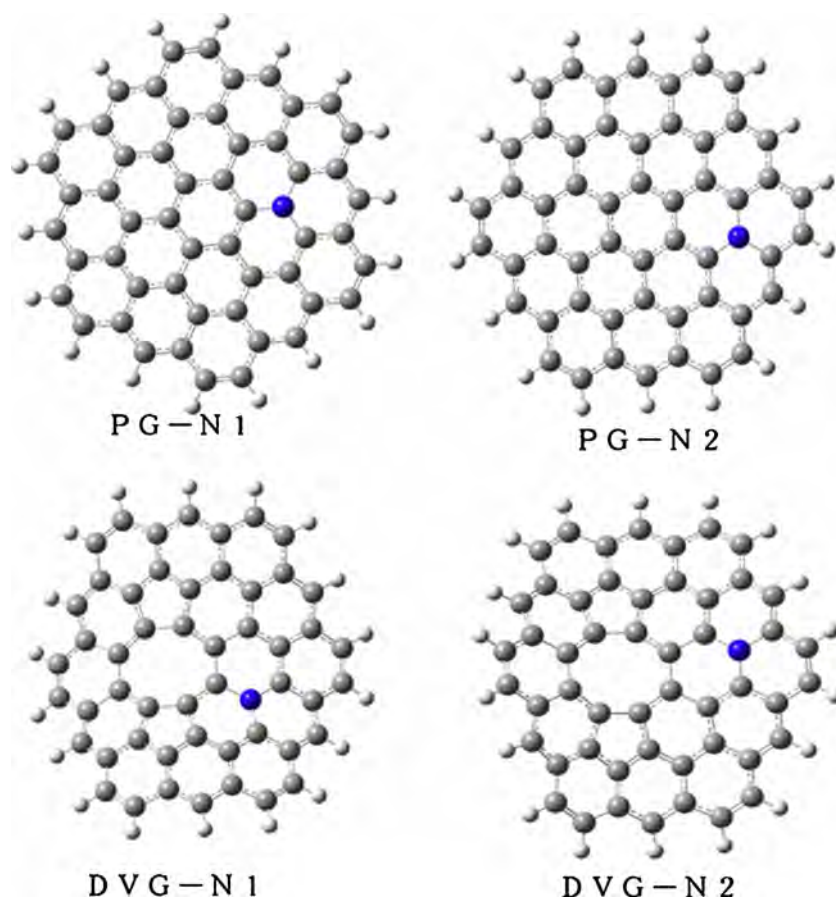


Fig. 7. The optimized structures of Carbon, nitrogen and hydrogen atoms are depicted in gray-green, blue and white (For interpretation of the references to colour in this figure legend, the reader is referred to the web version of this article).

as reported in the literature [36,37]. As shown in Fig. 10b, the mass loss of the fresh catalyst was less than the used catalysts in the temperature range of 100 °C to 450 °C. The mass loss of fresh C1100 was 6.38%, and that of the used catalyst was 12.24%. According to the above calculation method, the amount of coke deposition of C1100 was 5.86%, and this deposition occurred on the surface of the C1100 catalyst during acetylene hydrochlorination. Coke deposition may explain the C1100 catalyst deactivation and is consistent with results reported in the literature [38,39].

To remove the coke from the surface of the catalysts, used C1100

was regenerated by treating with  $NH_3$  at 700 °C for 1 h at a ramp rate of 5 °C/min.  $NH_3$  generates  $H_2$  and N species under high temperatures and removes the coke while preventing the loss of N species to recover the active sites [40–42]. As shown in Fig. 11, the catalytic activity of regenerated C1100 was 91% recovered, thus indicating that the C1100 catalyst could be easily regenerated after deactivation.

#### 4. Conclusions

In summary, we found that carbon defects in nitrogen-doped carbon

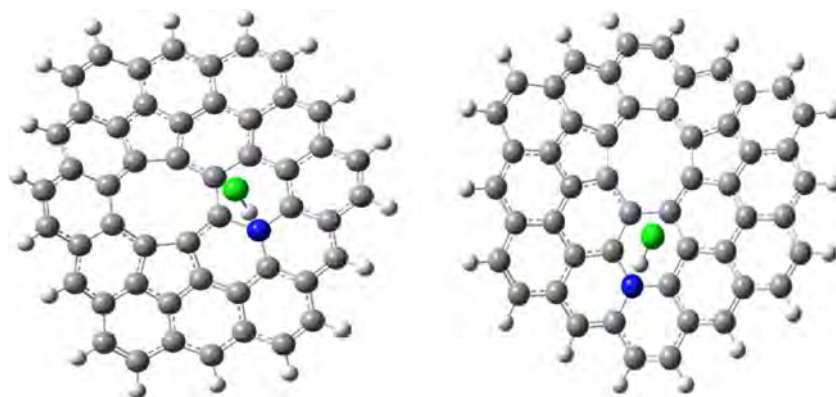


Fig. 8. The corresponding most stable adsorption structures of HCl.

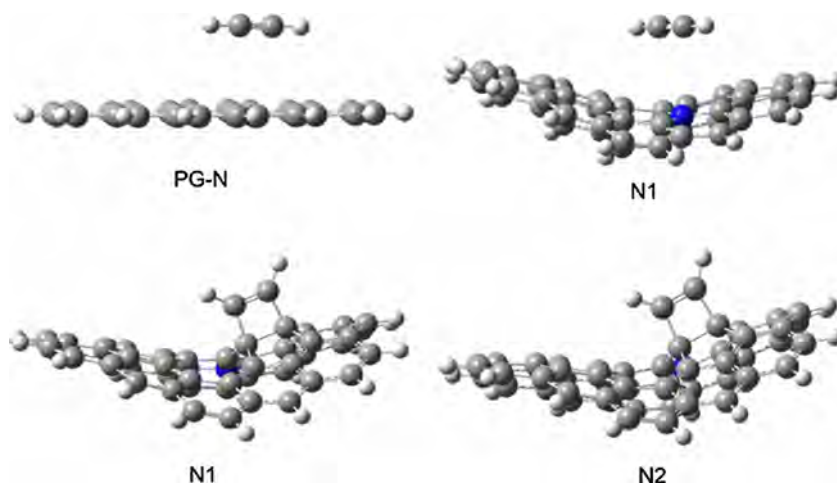


Fig. 9. The corresponding most stable adsorption structures of  $C_2H_2$ .

Table 3

The adsorption energies of  $C_2H_2$  and HCl adsorbed in PG-N, DVG-N1, and DVG-N2.

	PG-N (kcal/mol)	DVG-N1 (kcal/mol)	DVG-N2 (kcal/mol)
$C_2H_2$	−4.61	−6.45	−5.89
HCl	−3.24	−5.55	−5.07

could enhance the adsorption capacity of  $C_2H_2$  and HCl and promote acetylene hydrochlorination. The synthesised C1100 catalyst displayed excellent catalytic activity, close to that of a Au catalyst, under the reaction conditions of GHSV ( $C_2H_2$ ) = 36/h and 220 °C. The C1100 catalyst could be easily regenerated by treating with  $NH_3$  at 700 °C after deactivation. The relationship between the carbon defects and catalytic activity may be useful for designing better carbon-based catalysts for acetylene hydrochlorination.

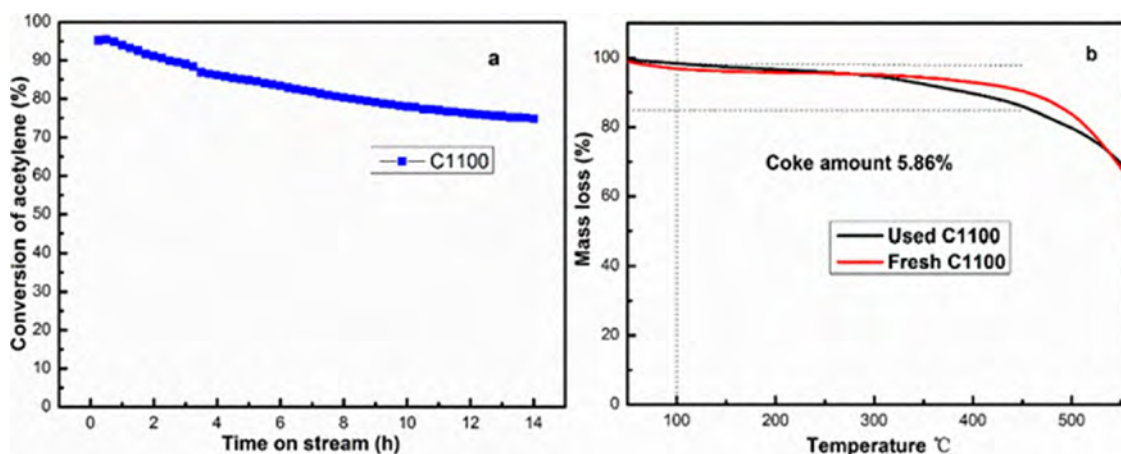


Fig. 10. (a): Stability test of C1100, Reaction conditions: under  $36\text{ h}^{-1}$  ( $C_2H_2$ ) and 220 °C; (b): Thermogravimetric analysis (TGA) curves recorded in oxygen atmosphere of fresh catalyst and spent C1100 catalyst.

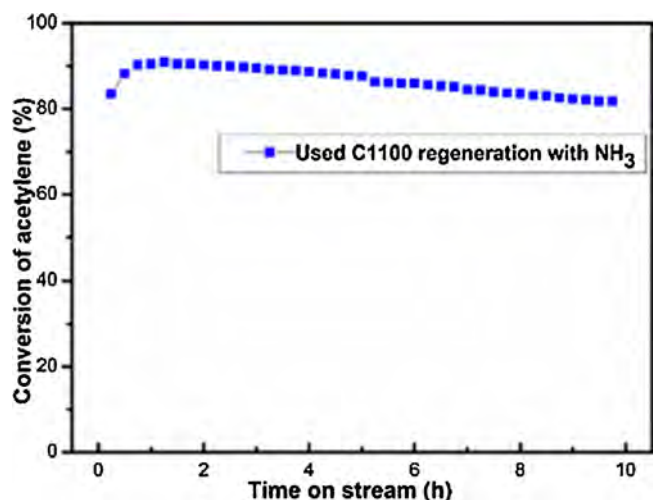


Fig. 11. The acetylene conversion of the used C1100 catalysts for acetylene hydrochlorination, conditions: under  $36 \text{ h}^{-1}$  ( $\text{C}_2\text{H}_2$ ) and  $220^\circ\text{C}$ .

### Acknowledgements

This work was supported by the National Natural Science Funds of China (NSFC, 21666033, U1403294), the Young Scientific and Technological Innovation Leader of Bingtuan (2015BC001), the State Key Research and Development Project of China (2016YFB0301603).

### References

- [1] B. Dai, X. Li, J. Zhang, F. Yu, M. Zhu, *Chem. Eng. Sci.* 135 (2015) 472–478.
- [2] H. Zhang, W. Li, X. Li, W. Zhao, J. Gu, X. Qi, Y. Dong, B. Dai, J. Zhang, *Catal. Sci. Technol.* 5 (3) (2015) 1870–1877.
- [3] H. Zhang, B. Dai, W. Li, X. Wang, J. Zhang, M. Zhu, J. Gu, *J. Catal.* 316 (7) (2014) 141–148.
- [4] K. Zhou, J. Jia, C. Li, H. Xu, J. Zhou, G. Luo, F. Wei, *Green Chem.* 17 (1) (2014) 356–364.
- [5] P. Johnston, N. Carthey, G.J. Hutchings, *J. Am. Chem. Soc.* 138 (23) (2016) 14548–14557.
- [6] X. Li, M. Zhu, B. Dai, *Appl. Catal. B-Environ.* 142 (5) (2013) 234–240.
- [7] M. Zhu, L. Kang, Y. Su, S. Zhang, B. Dai, *Can. J. Chem.* 91 (2) (2013) 120–125.
- [8] K. Zhou, B. Li, Q. Zhang, J.Q. Huang, G.L. Tian, J.C. Jia, M.Q. Zhao, G.H. Luo, D.S. Su, *F. Wei, ChemSusChem* 7 (3) (2014) 723.
- [9] X. Li, X. Pan, L. Yu, P. Ren, X. Wu, L. Sun, F. Jiao, X. Bao, *Nat. Commun.* 5 (1) (2014) 3688.
- [10] C. Zhang, L. Kang, M. Zhu, B. Dai, *RSC Adv.* 5 (10) (2015) 7461–7468.
- [11] B. Dai, K. Chen, Y. Wang, L. Kang, M. Zhu, *ACS Catal.* 5 (4) (2015) 2541–2547.
- [12] X. Zhao, X. Zou, X. Yan, C.L. Brown, Z. Chen, G. Zhu, X. Yao, *Inorg. Chem. Front.* 3 (3) (2016) 417–421.
- [13] C. Hu, L. Dai, *Angew. Chem. Int. Ed. English* 55 (39) (2016) 11736.
- [14] Y. Jiang, L. Yang, T. Sun, J. Zhao, Z. Lyu, O. Zhuo, X. Wang, Q. Wu, J. Ma, Z. Hu, *ACS Catal.* 5 (11) (2015) 6707–6712.
- [15] F. Zhao, L. Kang, *ChemistrySelect* 2 (21) (2017) 6016–6022.
- [16] H. Zhao, C. Sun, Z. Jin, D.W. Wang, X. Yan, Z. Chen, G. Zhu, X. Yao, *J. Mater. Chem. A-Chem.* 3 (22) (2015) 11736–11739.
- [17] J. Feng, B. Liang, D. Wang, H. Wu, L. Xue, X. Li, *Langmuir* 24 (19) (2008) 11209–11215.
- [18] M. J. Frisch, G. W. Trucks, H. B. Schlegel, G. E. Scuseria, M. A. Robb, J. R. Cheeseman, G. Scalmani, V. Barone, B. Mennucci, G. A. Petersson, H. Nakatsuji, M. Caricato, X. Li, H. P. Hratchian, A. F. Izmaylov, J. Bloino, G. Zheng, J. L. Sonnenberg, M. Hada, M. Ehara, K. Toyota, R. Fukuda, J. Hasegawa, M. Ishida, T. Nakajima, Y. Honda, O. Kitao, H. Nakai, T. Vreven, J. A. Montgomery Jr., J. E. Peralta, F. Ogliaro, M. Bearpark, J. J. Heyd, E. Brothers, K. N. Kudin, V. N. Staroverov, T. Keith, R. Kobayashi, J. Normand, K. Raghavachari, A. Rendell, J. C. Burant, S. S. Iyengar, J. Tomasi, M. Cossi, N. Rega, J. M. Millam, M. Klene, J. E. Knox, J. B. Cross, V. Bakken, C. Adamo, J. Jaramillo, R. Gomperts, R. E. Stratmann, O. Yazyev, A. J. Austin, R. Cammi, C. Pomelli, J. W. Ochterski, R. L. Martin, K. Morokuma, V. G. Zakrzewski, G. A. Voth, P. Salvador, J. J. Dannenberg, S. Dapprich, A. D. Daniels, O. Farkas, J. B. Foresman, J. V. Ortiz, J. Cioslowski, D. J. Fox, Gaussian Inc., Wallingford CT 2010.
- [19] Y. Zhao, D.G. Truhlar, *Theor. Chem. Acc.* 120 (1–3) (2008) 215–241.
- [20] S. Grimme, S. Ehrlich, L. Goerigk, *J. Comput. Chem.* 32 (7) (2011) 1456–1465.
- [21] S. Grimme, *J. Comput. Chem.* 27 (15) (2006) 1787–1799.
- [22] T. H. D Jr, *J. Chem. Phys.* 90 (2) (1989) 1007–1023.
- [23] C. Rungnim, R. Chanajaree, T. Rungrotmongkol, S. Hannongbua, N. Kungwan, P. Wolschann, A. Karpfen, V. Parasuk, *J. Mo. Model.* 22 (4) (2016) 85.
- [24] H. Qian, F. Han, B. Zhang, Y. Guo, J. Yue, B. Peng, *Carbon* 42 (4) (2004) 761–766.
- [25] Y. Kim, J. Ihm, E. Yoon, G.D. Lee, *Phys. Rev. B-Condens Matter* 84 (7) (2011) 2789.
- [26] M.M. Ugeda, I. Brihuega, F. Hiebel, P. Mallet, J.Y. Veuillen, J.M. Gómezrodríguez, F. Ynduráin, *Physics* 85 (12) (2012) 12–15.
- [27] X. Yan, Y. Jia, T. Odedairo, X. Zhao, Z. Jin, Z. Zhu, X. Yao, *Chem. Commun.* 52 (2016) 8156–8159.
- [28] M. Borghei, P. Kanninen, M. Lundahl, T. Susi, J. Sainio, I. Anoshkin, A. Nasibulin, T. Kallio, K. Tammesveski, E. Kauppinen, *Appl. Catal. B- Environ.* 158–159 (1) (2014) 233–241.
- [29] G. Wu, M. Nelson, S. Ma, H. Meng, G. Cui, P.K. Shen, *Carbon* 49 (12) (2011) 3972–3982.
- [30] X. Li, J. Zhang, W. Li, *J. Ind. Eng. Chem.* 44 (2016) 146–154.
- [31] K.L. Saenger, J.C. Tsang, A.A. Bol, J.O. Chu, A. Grill, C. Lavoie, *Appl. Phys. Lett.* 96 (15) (2010) 183.
- [32] M. Hu, J. Reboul, S. Furukawa, N.L. Torad, Q. Ji, P. Srinivasu, K. Ariga, S. Kitagawa, Y. Yamauchi, *J. Am. Chem. Soc.* 134 (6) (2012) 2864–2867.
- [33] N. Bozovic, I. Bozovic, J. Misewich, *Nano Lett.* 8 (12) (2008) 4477–4482.
- [34] D. Graf, F. Molitor, K. Ensslin, C. Stampfer, A. Jungen, C. Hierold, L. Wirtz, *Nano Lett.* 7 (2) (2006) 238–242.
- [35] X. Li, Y. Wang, L. Kang, M. Zhu, B. Dai, *J. Catal.* 311 (3) (2014) 288–294.
- [36] C. Huang, M. Zhu, L. Kang, X. Li, B. Dai, *Chem. Eng. J.* 242 (2014) 69–75.
- [37] H. Zhang, W. Li, Y. Jin, W. Sheng, M. Hu, X. Wang, J. Zhang, *Appl. Catal. B-Environ.* 189 (2016) 56–64.
- [38] J. Zhao, T. Zhang, X. Di, J. Xu, S. Gu, Q. Zhang, N.I. Jun, X. Li, *Catal. Sci. Technol.* 5 (11) (2015) 4973–4984.
- [39] S. Shang, W. Zhao, Y. Wang, X. Li, J. Zhang, Y. Han, W. Li, *ACS Catal.* 7 (5) (2017) 3510–3520.
- [40] X. Li, P. Li, X. Pan, H. Ma, X. Bao, *Appl. Catal. B-Environ.* 210 (2017) 116–120.
- [41] R.P. Lindstedt, F.C. Lockwood, M.A. Selim, *Combust. Sci. Technol.* 108 (4–6) (1995) 231–254.
- [42] M. Mrowetz, W. Balcerski, A.J. Colussi, M.R. Hoffmann, *J. Phys. Chem. B* 108 (108) (2004) 17269–17273.